Correlation of *In Vivo* Clot Deposition With the Flow Characteristics in the 50 cc Penn State Artificial Heart: A Preliminary Study

Pramote Hochareon,* Keefe B. Manning,* Arnold A. Fontaine,* John M. Tarbell,† and Steven Deutsch*

Flow stasis in an artificial heart may provide a situation where thrombus develops. Should part, or all, of the clot dislodge, a thromboembolism may lead to stroke(s), neurologic deficits, or even death. In an effort to determine if the regime of low shear or stasis exists, a two-dimensional particle image velocimetry (PIV) system was implemented to measure the velocity field within the 50 cc Penn State Artificial Heart. The velocity measurements were decomposed nearest the wall to obtain wall shear rates along the bottom of the chamber. The PIV measurements were made in three image planes across the depth of the chamber to reconstruct a surface distribution of the wall shear rates at the bottom over the entire heart cycle. The wall shear rate is shown to be spatially nonuniform, with persistently low wall shear rates. An area near the front edge of the chamber at the bottom showed wall shear rates not exceeding 250 s^{-1}. This was an area of clot formation seen *in vivo*, suggesting a link may exist between the low wall shear rate zone and thrombus formation. *ASAIO Journal* 2004; 50:537–542.

Yamanaka *et al.*[1] performed an *in vivo* study of the 50 cc Penn State artificial heart by implanting the device in three calves. The results show different patterns of clot depositions, (**Figure 1**). Most of the clots were tightly attached to the very back (**Figure 2**) of the sac in a region that could not be probed by particle image velocimetry (PIV). However, there was one narrow and long clot at the bottom, which extended to the outlet side and is shown in **Figure 1** on the outlet and bottom views. Unlike the majority of the clots, this clot was loosely attached to the surface, which is an indication that the shear stress in this region is low. We seek to determine in this study, then, whether the position of this clot is related to the local flow patterns at the bottom of the heart.

Under hemodynamic situations where elevated shear stresses result in hemolysis and platelet activation, areas of low shear, such as recirculation and stagnant zones, in combination with long residence times, become more prone to thrombus deposition and platelet aggregation.[2,3] Ryu *et al.*[4] have indicated, from measurements in an artificial heart, that some evidence exists linking low near wall velocities or flow separation to protein adsorption, which has been implicated in platelet adhesion.[5,6]

In a recent PIV study[7,8] over a single, near centerline plane, we reported that the bottom region of the 50 cc device experienced low shear over the entire pump cycle. We have also found,[9] however, that the diaphragm has a complex opening motion that influences the direction of the inflow jet. This implies that the single plane measurements previously reported might not be sufficient to define the flow field adequately. Therefore, in this study, we report measurements taken in three planes across the depth of the artificial heart chamber.

Methods

The 50 cc Penn State artificial heart test chamber was made of transparent Plexiglas with a refractive index of 1.48. It was machined to be identical to the geometry of the front half of the implantable 50 cc artificial heart. The rear part of the chamber is covered by a flexible, polyurethane diaphragm fabricated with the same material used in the implantable artificial heart sac. The pusher plate, which compressed the blood sac, was driven by a piston pump (Harvard Apparatus Co., Millis, MA). Bjork-Shiley (Shiley Inc., Irvine, CA) monostrut valves with pyrolytic carbon discs were used at the mitral (23 mm diameter) and aortic (21 mm diameter) ports, respectively, to achieve unidirectional flow.

To simulate physiologic conditions, the artificial heart experiments were performed with a mock circulatory loop.[10] The inlet and outlet compliance chambers simulated the atrial and aortic compliance, respectively, while a parallel plate resistor downstream of the aortic compliance simulated the systemic resistance. A reservoir between the systemic resistance and the atrial compliance controlled the preload to the chamber. Pressure waveforms at the inlet and outlet compliance chambers were monitored by pressure transducers (Maxxim Medical, Athens, TX). Two ultrasonic flow meters (Transonic System Inc., Ithaca, NY) were used to record the flow waveforms at the inlet and outlet ports. The stroke length was monitored through the pusher plate position as recorded by a linear velocity displacement transducer (Solartron Metrology, West Sussex, UK).

The blood analog fluid was a mineral oil (Penreco Inc.,

From the *Department of Bioengineering, Pennsylvania State University, University Park, Pennsylvania; and the †Department of Biomedical Engineering, The City College of New York, New York.

Submitted for consideration April 2004; accepted for publication in revised form August 2004.

This study was supported by NIH grant (HL60276).

Presented in part at the ASAIO 50th Anniversary Conference, Washington, DC, June 17–19, 2004.

Correspondence: Dr. Steven Deutsch, Department of Bioengineering, Pennsylvania State University, 205 Hallowell Building, University Park, PA 16802.

DOI: 10.1097/01.MAT.0000145694.40637.A0

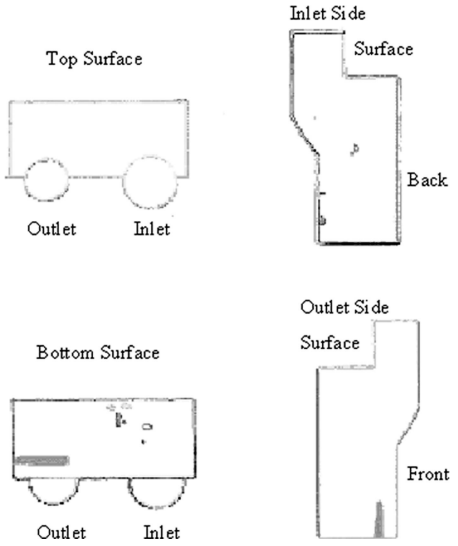

Figure 1. The clot depositions on the wall surfaces within the 50 cc chamber (results from two blood sacs implanted in two calves for 30 days, courtesy of Hanako Yamanaka).

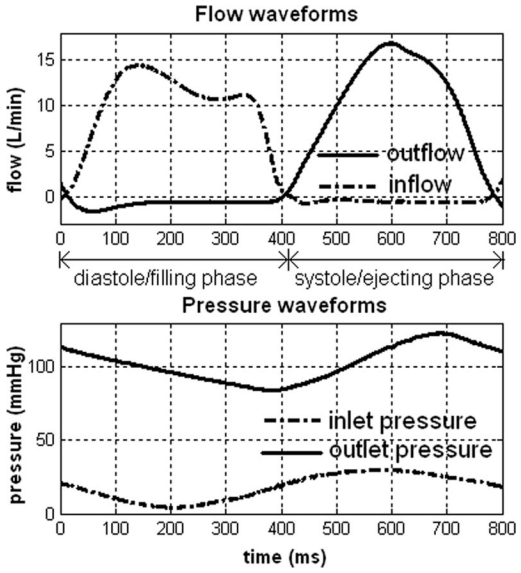

Figure 3. Inlet and outlet flow and pressure waveforms for the particle image velocimetry study.

Houston, TX), with a specific gravity of 0.827, refractive index of 1.46, and viscosity of 4.7 cP at room temperature. Red fluorescent 7 μm polystyrene particles (Duke Scientific Corp., Palo Alto, CA), with specific gravity of 1.055, were used for this experiment.

A dual pulsed Nd:YAG laser (New Wave Research, Fremont, CA) and appropriate cylindrical lens were used to form an approximately 1.5 mm thick light sheet to visualize the particles. A PIV synchronizer (TSI Inc., St. Paul, MN) with frame grabber board (TSI Inc.) was used. PIV image pairs were recorded by a 1,024 × 1,018 CCD camera (TSI, Inc.) for each velocity field. The time marker for each beat cycle was referred to the pusher plate position to minimize the beat to beat uncertainty of the time reference. An external triggering signal was generated by a signal delay toolbox, which has a time increment of 0.1 ms.

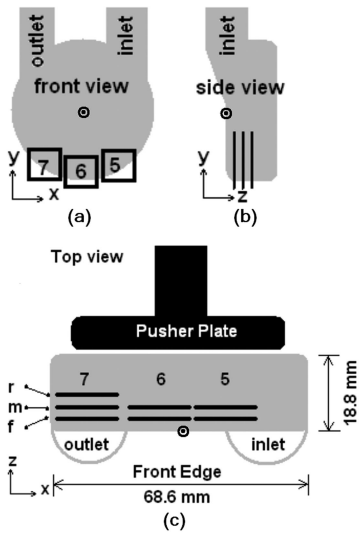

Figure 2. Geometric orientation of the PIV measurement planes: (a) in X-Y plane, (b) Z locations: 3 mm, 6 mm, and 9 mm from the frontal edge (frontal, middle, and rear planes, respectively), and top view illustrates the 50 cc chamber dimensions with PIV plane locations. The dot with a circle around it indicates the origin of the coordinate axes on all three graphic representations. The figures are not drawn to scale. A short notation for the planes begins with the letter (f = frontal plane, m = middle plane, and r = rear plane) indicating Z location and is followed by the number (5, 6, and 7) indicating the chamber area in the X axis (for example, F-7. F = all the measurement views in frontal plane: F-7, F-6, and F-5; series 7 = all the measurement views at area 7: F-7, M-7, and R-7). PIV, particle image velocimetry.

For this study, PIV measurements were made at the bottom of the chamber in the three measurement areas shown in **Figure 2**. The overall image magnification was approximately 10 μm/pixel, and wall shear could be estimated from velocities as close as 160 μm from the wall. As shown in **Figure 2**, the measurement planes were shifted along the depth of the 18 mm wide chamber to capture the off centerline characteristics of the flow. Note that because of the nonuniformity of the sac opening, the rear planes for locations 5 and 6 were blocked by the diaphragm, preventing data acquisition in those regions. All velocity maps were ensemble averaged from 200 instantaneous velocity fields at each location and for each time. The PIV processing is given in detail in Hochareon *et al.*[7] and summarized here.

Cross-correlation of the images was performed by the TSI Insight 5 software. A recursive or multigrid cross-correlation scheme was used with an initial interrogation window of 64 × 64 pixels, stepped down by a factor of two to reach the final interrogation window of 16 × 16 pixels.[11,12] The final 16 × 16 pixel interrogation size was selected to achieve a minimum of four particles per interrogation window[13–15] and an optimal interrogation window size for first order accurate wall shear rate calculations, as based upon earlier results.[7] A Hart cross-correlation based correction, with sparse array compressed image correlation,[16–18] was selected with a bilinear peak finding algorithm. Each interrogation window has 50% overlapping with its neighbors. Nonfluid areas were digitally masked

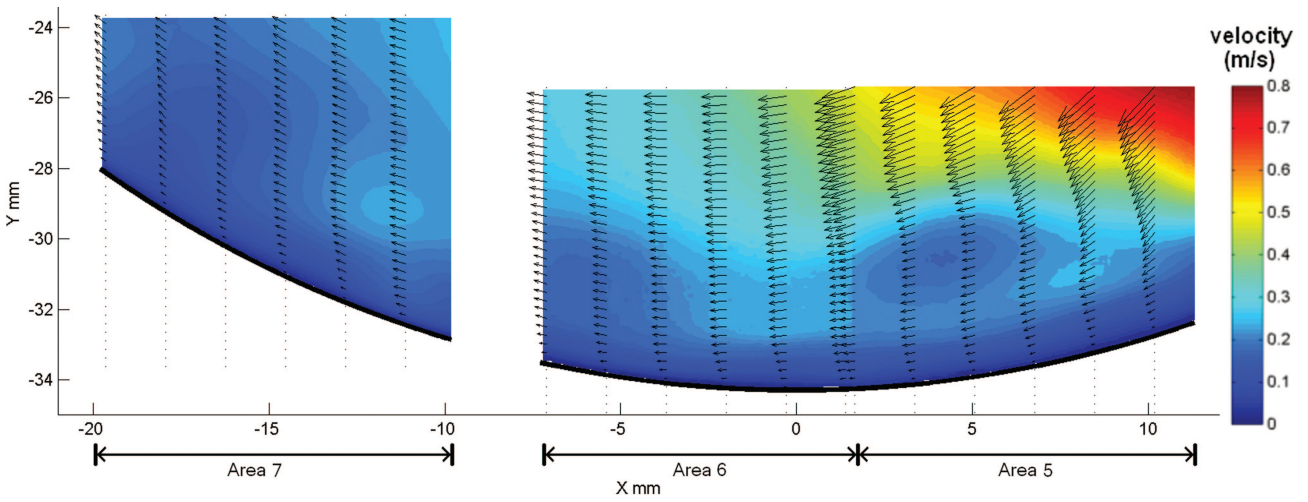

Figure 4. Ensemble average velocity map of areas 5, 6, and 7 (indicated by brackets along the X axis) in the middle plane during early diastole at 100 ms.

to prevent anomalies in the Plexiglas model from influencing the cross-correlation.[8]

A range and local median validation criteria[19] were sequentially used for each vector file obtained from Insight 5. The exact tolerance values (approximately 80%) for each criterion were manually adjusted to obtain reasonable results. Invalid instantaneous vectors were manually excluded. For the remaining valid vector files, no interpolation and no smoothing has been applied to avoid error propagation from neighboring vectors.

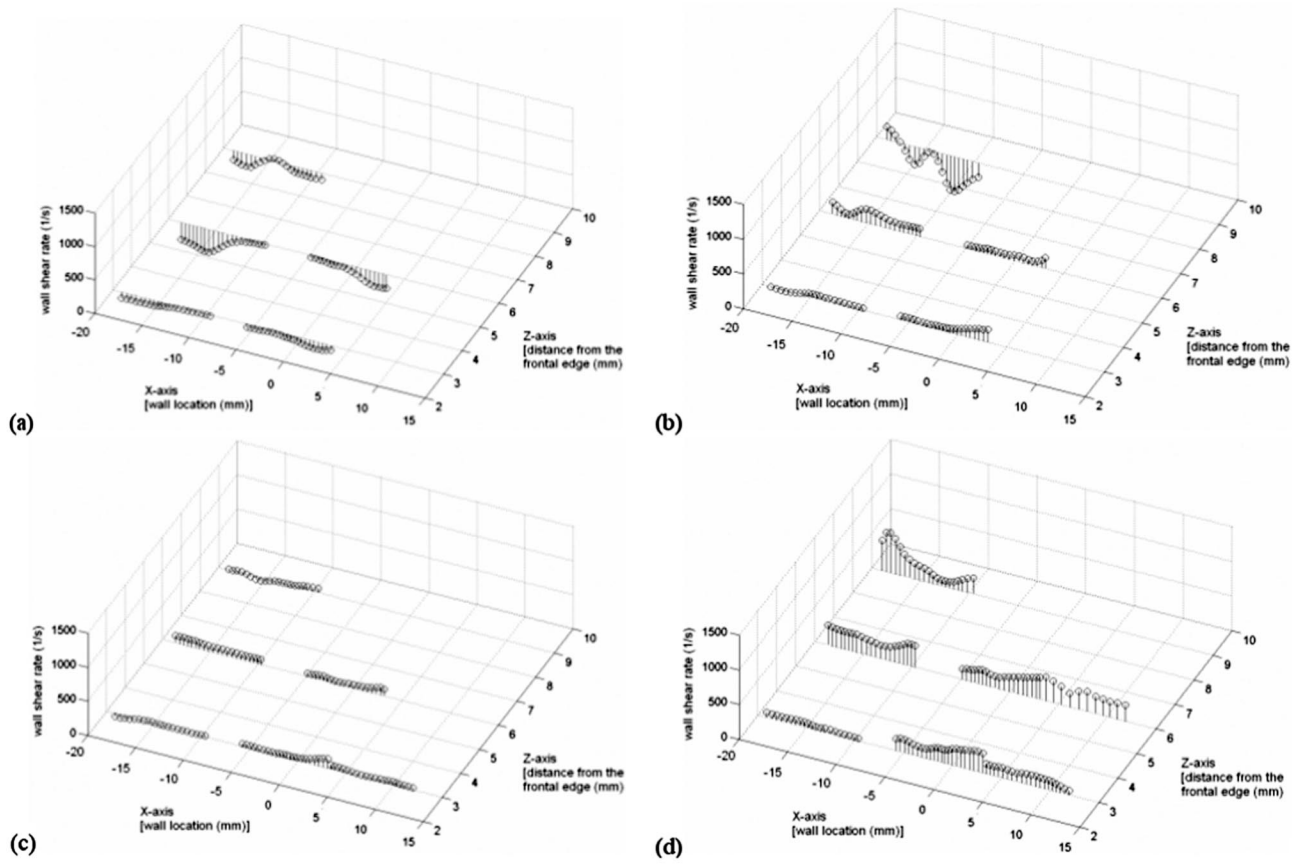

Figure 5. Wall shear rate distribution on the 50 cc chamber's bottom surface during the onset of diastole (the sign of the presented shear rates is reversed for visualizing purposes): (a) 0 ms, (b) 25 ms, (c) 50 ms, and (d) 100 ms.

Averaging was performed vector by vector to obtain the ensemble mean velocity field as a function of space and time.

Wall shear rate calculations were performed by a wall coordinate decomposition of the near wall velocity vectors and a first order, one sided forward differencing of the tangential velocity component, in conjunction with the no slip boundary condition at the wall. A dT of 75 to 200 μs was used to ensure a sufficient number of particles within each interrogation region. The u velocity ($u = \Delta x/dT$) was decomposed locally (with respect to the wall) into normal and tangential components. The tangential velocity was divided by the orthogonal distance to the wall. Further details of the wall shear rate calculation may be found in Hochareon *et al.*[7]

In vitro experimental operating conditions were an average flow rate of 4.72 L/min, stroke length of 19.4 mm, stroke volume of 62.93 cc, and heart rate of 75 bpm.

To briefly summarize the *in vivo* data methods, 50 cc devices were implanted in three calves for 30 days as ventricular assist devices. The overall average flow rate was approximately 3.13 L/min. The animals were under an anticoagulant therapy regimen. The clot depositions given in **Figure 2** are a composite picture of the results from the three calves. Further details may be found in Yamanaka *et al.*[1]

Results

The measured, near physiologic flow and pressure waveforms for this work are shown in **Figure 3**. Diastole is from 0 to 430 ms, whereas systole is from 430 ms to the end of the cycle at 800 ms.

A major feature of the bottom flow field is the penetration of the inlet jet in early (100 ms) diastole, as shown in **Figure 4** covering areas 5, 6, and 7. This inlet jet is responsible for setting up the clockwise rotational, wall washing motion, observed first by Baldwin *et al.*[20] The maximum velocity at the bottom of the chamber is approximately 0.8 m/s and is associated with the inlet jet. During early diastole, a thick boundary layer, typical of a low shear region, forms. Although the inflow jet is observed to wander in time, the flow structures in all three planes are not vastly different,[7] so that we treat the flow as essentially two-dimensional for the purpose of shear rate calculations. By comparison with simulations,[8] we can estimate the wall shear rate uncertainty at no more than ± 20%.

Figures 5 to 7 illustrate the wall shear rate distribution on the bottom surface, as a function of cycle time, for the entire beat cycle of the pump. The x-z plane of the plots corresponds to that in **Figure 2**. The sign of the wall shear rates is reversed in these figures to help with the visualization so that a negative wall shear rate corresponds to flow in the clockwise direction.

Discussion

From **Figure 5a**, for very early diastole, we note that the shear rates are generally low and indicate a counter clockwise flow pattern in the middle and rear planes. This occurs when

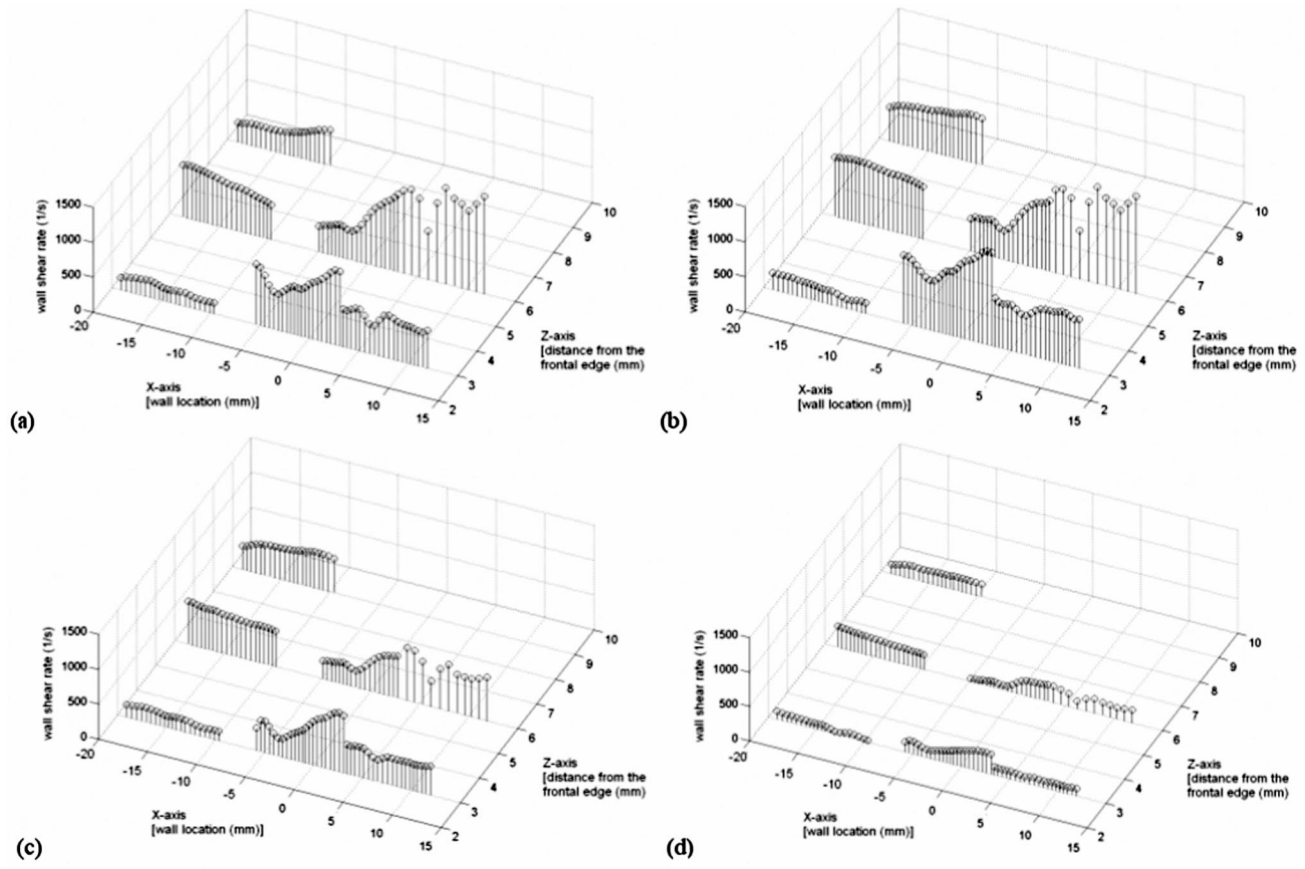

Figure 6. Wall shear rate distribution on the 50 cc chamber's bottom surface during diastole (200–400 ms) and early systole (500 ms) (the sign of the presented shear rates is reversed for visualizing purposes): (a) 200 ms, (b) 300 ms, (c) 400 ms, and (d) 500 ms.

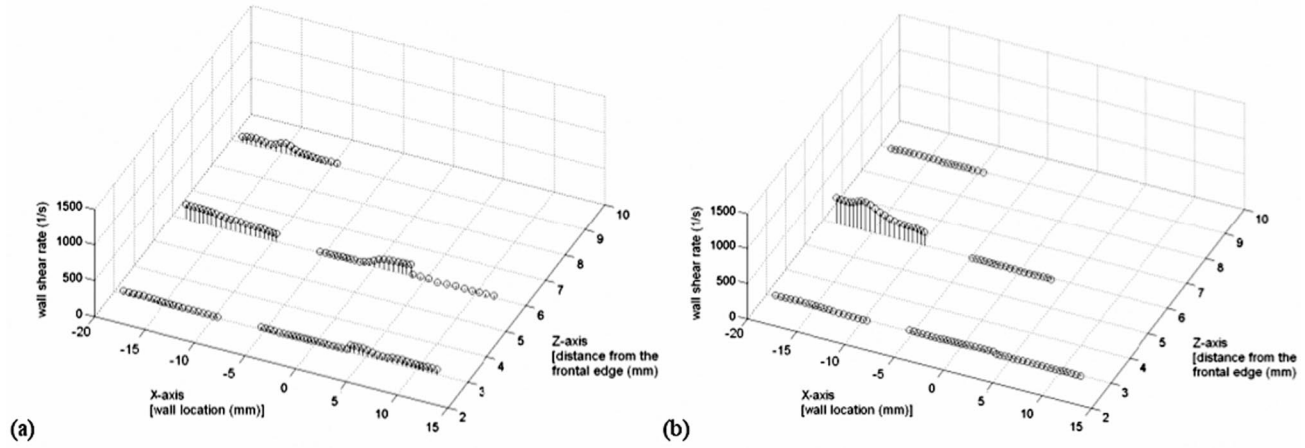

Figure 7. Wall shear rate distribution on the 50 cc chamber's bottom surface during mid to late systole (the sign of the presented shear rates is reversed for visualizing purposes): (a) 600 ms and (b) 700 ms.

the pusher plate is pulling back from the front edge and the cross plane component of velocity may be strong. At the time that the inflow jet reaches the bottom, near 100 ms, the flow is clockwise and the wall shear rates have increased in magnitude in the direction of the flow. It is clear (see for example, **Figure 5d**) that the shear rate profile is not uniform across the bottom of the chamber. Note, in particular, the nearly zero shear rate in region F-7 located 3 mm from the 50 cc front wall, as shown in **Figure 5**. This location coincides with the loose clot found *in vivo*.

Figure 6 shows the shear rate profiles from mid diastole through early systole. The wall shear rates peak near at 1,500 s^{-1} in mid diastole (**Figure 6b**) and then subside. Again the shear rate profiles are not uniform across the bottom surface and region F-7 is an area of very low shear rate throughout. As shown in **Figures 6d and 7**, systole is a period of generally low wall shear rate for the entire bottom surface.

In previous studies using laser Doppler anemometry (LDA), Baldwin *et al.*[20] measured Reynolds stresses as high as 20,000 dynes/cm^2 in the regurgitant jet of a Bjork-Shiley Monostrut mitral valve, indicating hemolysis was likely to occur because of the regurgitant flow. While investigating three phases of the mechanical heart valve cycle, Lamson *et al.*[21] also indicated that the backward flow (regurgitant flow) produced an index of hemolysis comparable with the forward flow even though the overall backward flow rate is 2 to 5% of the forward flow rate. Sallam and Hwang[22] showed hemolysis occurred past a threshold of 4,000 dynes/cm^2 through a tilting disc heart valve during an exposure time of 1 ms. In addition, Bluestein *et al.*[23] have shown that platelet activation occurs during mechanical heart valve closure. Since some platelets have been activated because of the mechanical heart valve and the area along the bottom of the chamber (F-7) experiences very low wall shear rates (no more than 250 s^{-1}) over the entire cycle, thrombus formation would seem likely to develop in that region as such thrombi have been seen *in vivo*.

Conclusion

Particle image velocimetry was used to measure three image planes within the 50 cc Penn State Artificial Heart to obtain the velocity flow fields. Using PIV, we have introduced a technique that can produce the wall shear rate inside the entire artificial heart quite rapidly. In this study, we have shown that low wall shear rates exist along the bottom of the chamber over a large part of the heart cycle. Specifically, an area near the front wall along the bottom of the chamber experiences wall shear rates below 250 s^{-1}. In combination with hemolysis and platelet activation, known to occur with mechanical heart valves, this area would be quite susceptible to thrombus formation. Yamanaka *et al.*[1] found a loose clot during *in vivo* work with the 50 cc Penn State Artificial Heart in the region where we measured near zero shear rate throughout the pump cycle. Although we can certainly not conclude that the loose clot that formed was caused by the low shear rate, the correlation of these results is intriguing. Additional work along these lines is continuing. The PIV approach we have developed provides the investigator with an opportunity to use *in vitro* measurements as an integral part of the design process. For example, one might speculate that the stagnant flow near the bottom region is a result of the angling of the inlet valve 30° (as is the case here) and carry out a parametric study of valve angle against shear rate using PIV.

References

1. Yamanaka H, Rosenberg G, Weiss WJ, *et al*: A multiscale surface evaluation of thrombosis in left ventricular assist systems. *ASAIO J* 49: 222, 2003.
2. Turitto VT, Hall CL: Mechanical factors affecting hemostasis and thrombosis. *Thromb Res* 92: S25–S31, 1998.
3. Wootton DM, Ku DN: Fluid mechanics of vascular systems, diseases, and thrombosis. *Annu Rev Biomed Eng* 1: 299–329, 1999.
4. Ryu GH, Kim J, Chang JK, *et al*: The fluid dynamic effect on protein adsorption in left ventricular assist devices. *ASAIO J* 39: M332–M336, 1993.
5. Kim J, Ryu G, Shin I, *et al*: Effect of shear rates on protein adsorption in the total artificial heart. *ASAIO J* 38: M532–M535, 1992.
6. Mandrusov E, Puszkin E, Vroman L, Leonard EF: Separated flows in artificial organs. A cause of early thrombogenesis? *ASAIO J* 42: M506–M513, 1996.
7. Hochareon P, Manning KB, Fontaine AA, Tarbell JM, Deutsch S:

Wall shear-rate estimation within the 50cc Penn State Artificial Heart using particle image velocimetry. *ASME J Biomech Eng* 126: 430–437, 2004.
8. Hochareon P: *Development of Particle Image Velocimetry (PIV) for Wall Shear Stress Estimation within a 50cc Penn State Artificial Heart Ventricular Chamber*. PhD Thesis, Pennsylvania State University: University Park, PA, 2003.
9. Hochareon P, Manning KB, Fontaine AA, Deutsch S, Tarbell JM: Diaphragm motion affects flow patterns in an artificial heart. *Artif Organs* 27: 1102–1109, 2003.
10. Rosenberg G: *A Mock Circulatory System for In Vitro Studies of Artificial Hearts*. MS Thesis, Pennsylvania State University: University Park, PA, 1972.
11. Scarano F, Riethmuller ML: Iterative multigrid approach in PIV image processing with discrete window offset. *Exp Fluids* 26: 513–523, 1999.
12. Scarano F, Riethmuller ML: Advances in iterative multigrid PIV image processing. *Exp Fluids* 29: S51–S60, 2000.
13. Raffel M, Willert CE, Kompenhans J: *Particle Image Velocimetry: A Practical Guide*. Berlin: Springer-Verlag, 1998.
14. Keane RD, Adrian RJ: Theory of cross-correlation analysis of PIV images. *App Scientific Res* 49: 191–215, 1992.
15. Adrian RJ: Particle imaging techniques for experimental fluid-mechanics. *Annu Rev Fluid Mech* 23: 261–304, 1991.
16. Hart DP: High-speed PIV analysis using compressed image correlation. *ASME J Fluids Eng* 120: 463–470, 1998.
17. Hart DP: Super-resolution PIV by recursive local-correlation. *J Visualization* 10: 1–10, 1999.
18. Hart DP: The elimination of correlation errors in PIV processing, in *9th International Symposium on Applications of Laser Techniques to Fluid Mechanics*. Lisbon, Portugal, 1998.
19. Westerweel J: Efficient detection of spurious vectors in particle image velocimetry data. *Exp Fluids* 16: 236–247, 1994.
20. Baldwin JT, Deutsch S, Geselowitz DB, Tarbell JM: LDA measurements of mean velocity and Reynolds stress fields within an artificial heart ventricle. *ASME J Biomech Eng* 166: 190–200, 1994.
21. Lamson TC, Rosenberg G, Geselowitz DB, *et al*: Relative blood damage in the three phases of a prosthetic heart valve flow cycle. *ASAIO J* 39: M626–M633, 1993.
22. Sallam AM Hwang NHC: Human red blood cell hemolysis in a turbulent shear flow: contribution of Reynolds shear stress. *Biorheology* 21: 783–797, 1984.
23. Bluestein D, Yin W, Affeld K, Jesty J: Flow-induced platelet activation in mechanical heart valves. *J Heart Valve Dis* 13: 501–508, 2004.